Hydrogen de/resorption properties of the LiBH4–MgH2–Al system

ARTICLE *in* THE JOURNAL OF PHYSICAL CHEMISTRY C · DECEMBER 2009

Impact Factor: 4.77 · DOI: 10.1021/jp9068366

Hydrogen De/Resorption Properties of the $LiBH_4-MgH_2-Al$ System

Yao Zhang,*,† Qifeng Tian,‡,§ Hailiang Chu,|| Jian Zhang,† Lixian Sun,† Juncai Sun,⊥ and Zhongsheng Wen⊥

Materials and Thermochemistry Group, Laboratory of Catalysis and New Materials for Aerospace, Dalian Institute of Chemical Physics, Chinese Academy of Sciences, Dalian 116023, China, Key Laboratory for Green Chemical Process of Ministry of Education, Wuhan Institute of Technology, Wuhan 430073, China, Hubei Key Laboratory of Novel Reactor and Green Chemical Technology, Wuhan Institute of Technology, Wuhan 430073, China, Complex Hydride Materials Research Group, Dalian Institute of Chemical Physics, Chinese Academy of Sciences, Dalian 116023, China, and Department of Materials Science and Engineering, Dalian Maritime University, Dalian 116026, China

Received: July 19, 2009; Revised Manuscript Received: November 17, 2009

The synthesized $LiBH_4-MgH_2-Al$ (4:1:1 mole ratio) composite exhibits reversible de/rehydrogenation properties. Thermogravimetry and differential scanning calorimetry indicate that the dehydrogenation onset temperature is reduced by 100 K from that of $2LiBH_4-MgH_2$ and $2LiBH_4-Al$ systems. The major dehydrogenation pathway for the $4LiBH_4-MgH_2-Al$ complex system can be identified as $4LiBH_4 + MgH_2 + Al \rightarrow 4LiH + MgAlB_4 + 7H_2$ by means of X-ray diffraction (XRD) measurements on the as-dehydrogenated samples. The isothermal dehydrogenation measurements exhibit that the maximum dehydrogenation amount (9.4 wt % H_2, 673 K) approaches the theoretical value (9.9 wt % H_2) of the reaction. Through pressure−composition isotherms ($P-C-T$) and the van't Hoff equation, the dehydrogenation enthalpy and entropy of the $4LiBH_4-MgH_2-Al$ system can be determined as 57 kJ/mol-H_2 and 75 J/K·mol-H_2, respectively. The system is slightly destabilized from pristine $LiBH_4$ ($\Delta H^{\circ}_{de} = 68$ kJ/mol-H_2) by coadditives of MgH_2 and Al. The XRD measurements on the rehydrogenated samples suggest that the above reaction is partially reversible and the backward reaction takes place in two steps as $4LiH + MgAlB_4 + 6H_2 \rightarrow Mg + 4LiBH_4 + Al$ and $Mg + H_2 \rightarrow MgH_2$. Because of the alloying of Mg with Al, MgH_2 in the complex system cannot be fully recovered below the temperature of 673 K. The isothermal rehydrogenation measurements exhibit significantly enhanced kinetics for the $LiH-MgAlB_4$ system compared with $LiH-MgB_2$ and $LiH-AlB_2$ systems.

1. Introduction

Considerable attention has been recently focused on such lightweight hydrogen storage materials as alanates and borohydrides due to their large hydrogen capacities. These so-called complex hydrides containing low-atomic-weight metal cations and anions of alanate (AlH_4^-), amide (NH_2^-), or borohydride (BH_4^-)[1–9] have high gravimetric and volumetric capacities for hydrogen. They are, at present, one of the most promising hydrogen storage materials for mobile applications based on hydrogen fuel cell techniques.

$LiBH_4$ is a potential complex hydride, owing to its large theoretical hydrogen capacity (18.5 wt %) and efficient capacity (13.8 wt %).[10] Unfortunately, the practical application of such a hydride in a mobile fuel cell system is limited due to both thermodynamic and kinetic deficiencies. It was observed that, after the $LiBH_4$ melts at approximately 553 K, the dehydrogenation reaction starts slowly from the liquid state (above 673 K) to generate a material mixture of boron and lithium hydride as per the following equation:[11]

$$LiBH_4 \rightarrow LiH + B + \frac{3}{2}H_2 \qquad (1)$$

The complete recombination of $LiBH_4$ with whole hydrogen content (18.5 wt %) remains difficult due to the inactive elemental boron, which might be realized at very high temperatures (above 873 K) and under extremely high pressure (35 MPa).[12]

Recently, many efforts are focused on doping additives, for example, metals,[13,14] metal halides,[15,16] oxides,[11] amides,[17,18] metal hydrides,[19–22] or nanoporous materials,[23,24] to lower the dehydrogenation temperature (T_{de}) and enhance the reversibility. Remarkable progress was achieved by Vajo and Skeith using MgH_2.[19] Especially, a molar ratio of 2:1 for $LiBH_4-MgH_2$ results in a novel pathway that is distinct from the self-decomposition in eq 1.

$$2LiBH_4 + MgH_2 \rightarrow 2LiH + MgB_2 + 4H_2 \qquad (2)$$

In eq 2, an 8−10 wt % reversible storage capacity was achieved. More importantly, the favorable formation of MgB_2 effectively stabilizes the dehydrogenated state and results in an overall 27 kJ/mol H_2 decrease in ΔH for eq 2 in comparison with eq 1.[19] The strategy stimulated extensive explorations on the reactions of $LiBH_4$ with some additives to obtain more metal borides, for example, AlB_2 and[22,26] CaB_6.[22,25,27] Among these composite systems, Al-doped $LiBH_4$ exhibits improved perfor-

* To whom correspondence should be addressed. Tel: 86-411-84379215. Fax: 86-411-84379213. E-mail: zhangyao@dicp.ac.cn.
† Laboratory of Catalysis and New Materials for Aerospace, Dalian Institute of Chemical Physics, Chinese Academy of Sciences.
‡ Key Laboratory for Green Chemical Process of Ministry of Education, Wuhan Institute of Technology.
§ Hubei Key Laboratory of Novel Reactor and Green Chemical Technology, Wuhan Institute of Technology.
|| Complex Hydride Materials Research Group, Dalian Institute of Chemical Physics, Chinese Academy of Sciences.
⊥ Dalian Maritime University.

10.1021/jp9068366
Published on Web 12/09/2009

mance of reversible hydrogen storage.[13,14,22,26] The reaction was suggested as follows:

$$2LiBH_4 + Al \rightarrow 2LiH + AlB_2 + 3H_2 \quad (3)$$

These advances mainly focus on specific aspects of $LiBH_4$-relevant systems, for example, enhanced kinetics[14] in a $LiBH_4-Al$ system or lowered thermal stability[19] in a $2LiBH_4-MgH_2$ system. The motivation of the work is to synthesize a $4LiBH_4-MgH_2-Al$ ternary component system and comprehensively optimize its hydrogen de/resorption properties through combining the reactions of eqs 2 and 3. Furthermore, the study would present a primary insight into the reactions occurring in the system and their influences on the performances of a $LiBH_4$-relevant composite. Thermogravimetric (TG) and differential scanning calorimetric (DSC) measurements were applied to investigate the nonisothermal dehydrogenation performance. The isothermal de/rehydrogenation measurements were carried out to study the reversible kinetics. X-ray diffraction (XRD) characterizations and Fourier transform infrared spectrometry (FT-IR) analyses were performed on the samples obtained at different temperatures ($T = 573$, 623, and 673 K) to identify the product phases. The thermodynamic property of the system was characterized by isothermal pressure−composition ($P-C-T$) measurements.

2. Experimental Section

Commercial $LiBH_4$ (95%, Alfa Aesar), Al (99%, Tianjin Delan), and MgH_2 (99%, Alfa Aesar) powders were directly used without further purification. The $4LiBH_4-MgH_2-Al$ mixture was ground in a QM-1SP planetary ball mill for 20 h at a rate of 500 rpm. In each stainless steel milling pot (100 mL), the ball-to-powder weight ratio was 50:1 and the protection atmosphere was 0.1 MPa Ar. All handlings of the sample were operated in a glovebox (MBraun unilab) filled with high-purity Ar (99.9999%) and low-density H_2O and O_2 (both <0.1 ppm).

TG measurements were executed upon a TherMax 500 (Thermo Cahn) from room temperature to 873 K with an argon purge rate of 50 mL/min. They were all performed at a heating rate of 10 K/min. The outlet gaseous species, including H_2, O_2, N_2, H_2O, and B_2H_6, were monitored using mass spectroscopy (MS, InProcess instrument). The profiles were obtained by monitoring the species with a mass-to-charge ratio of 2 (H_2^+), 17 (OH^+), 18 (H_2O^+), 27 ($B_2H_6^+$), 28 (N_2^+), 32 (O_2^+), and 40 (Ar^+). We carried out the DSC measurements using a Netzsch STA 409C with the same heating rate and argon purge rate as those of the TG measurements. The test temperature is within the range of 300−850 K.

The isothermal dehydrogenation kinetics was measured by a Sievert-type apparatus (Advanced Materials Corporation) under a background pressure of 100 Pa H_2. After dehydrogenation at 673 K, the isothermal rehydrogenation kinetics was carried out on the samples at various temperatures ($T = 573$, 623, and 673 K) with an initial pressure of 4 MPa H_2. Still on the apparatus, the pressure−composition isotherm ($P-C-T$) measurements were carried out at temperatures of 573, 623, and 673 K. The test pressure was within the range of 0.01−5 MPa.

XRD measurements on a PANalytical X'pert diffractometer (Cu Kα, 50 kV, 200 mA) were carried out to identify the product phases in the sample after de/rehydrogenation at different temperatures. We analyzed the phases and their structures by means of the databases in X'pert HighScore (version 2.2a) and PCPDFWIN (version 2.02). The vibration spectra of the species were identified using a Thermo-Fisher Fourier transform infrared spectrometer (FT-IR). The obtained samples were pressed with potassium bromide (KBr) powder at a weight ratio of 1:99 to form a pellet. The measurements adopt transmission mode.

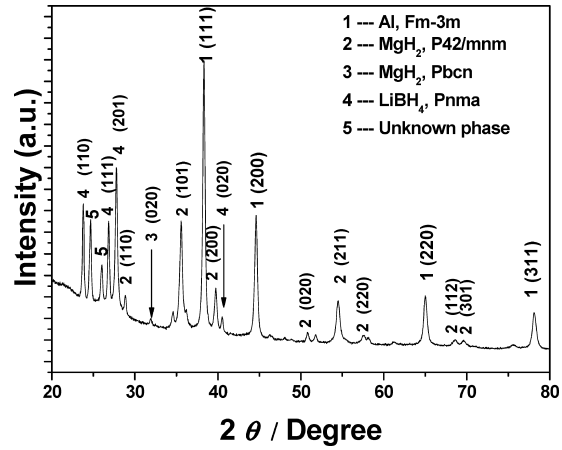

Figure 1. XRD pattern for the $4LiBH_4-MgH_2-Al$ system after ball-milling.

3. Results and Discussion

3.1. Dehydrogenation of the $LiBH_4-MgH_2-Al$ System. Figure 1 exhibits the XRD pattern for the $4LiBH_4-MgH_2-Al$ composite sample after 20 h of ball-milling. No reaction product among $LiBH_4$, MgH_2, and Al can be found in the mixture, indicating that the reactions among the initial phases do not occur during the preparation. It confirms that the as-milled sample is merely the physical mixture of the three phases. The unidentified reflections in the XRD patterns likely represent some intermediate phases resulted from partial self-decomposition of $LiBH_4$.[28]

Figure 2 shows nonisothermal dehydrogenation performances of the $LiBH_4-MgH_2-Al$ (4:1:1 mole ratio), $LiBH_4-MgH_2$ (2:1 mole ratio), and $LiBH_4-Al$ (2:1 mole ratio) samples tested by TG−MS and DSC measurements. The TG curves indicate that the onset temperature of $4LiBH_4-MgH_2-Al$ is reduced by ~100 K from the latter samples. DSC curves in Figure 2 reflect the thermodynamic behaviors of the $LiBH_4-MgH_2-Al$ (4:1:1 mole ratio), $LiBH_4-MgH_2$ (2:1 mole ratio), and $LiBH_4-Al$ (2:1 in mole ratio) samples. The endothermic peak corresponding to a major dehydrogenation of $4LiBH_4-MgH_2-Al$ shifts to a lower temperature by ~100 K in comparison with the $2LiBH_4-MgH_2$ and $LiBH_4-Al$ samples. The MS measurement was used to monitor the liberated gas from the TG measurement of the ball-milled $LiBH_4-MgH_2-Al$ mixture. The MS curves relevant to nitrogen, oxygen, water, and diborane are flat lines. Only the curve corresponding to hydrogen can be significantly detected, indicating that hydrogen is the only gaseous species released during the dehydrogenation process.

Figure 3 compares the isothermal kinetics for the species of $4LiBH_4-MgH_2-Al$, $2LiBH_4-MgH_2$, and $2LiBH_4-Al$. It shows that the saturated dehydrogenation process for the $4LiBH_4-MgH_2-Al$ sample can be limited within 3000 s, which is similar to that of $2LiBH_4-Al$ (~3000 s) but much lower than that of $2LiBH_4-MgH_2$ (≥7000 s). Importantly, the maximum dehydrogenation capacity of $4LiBH_4-MgH_2-Al$ (9.4 wt % H_2, 673 K) is higher than that of the $2LiBH_4-MgH_2$ (8 wt % H_2, 673 K) and $2LiBH_4-Al$ (6.5 wt % H_2, 673 K) samples. The capacity (9.4 wt % H_2, 673 K) approaches the theoretical value (9.9 wt % H_2) of the amalgamated reaction of eqs 1 and 2, which can be suggested as follows:

$$4LiBH_4 + MgH_2 + Al \rightarrow 4LiH + MgB_2 + AlB_2 + 7H_2 \quad (4)$$

To verify the existence of the hypothesized reaction, we executed an XRD analysis on the samples that were achieved after the isothermal dehydrogenation at various temperatures (573, 623, and 673 K), as shown in Figure 4. However, neither

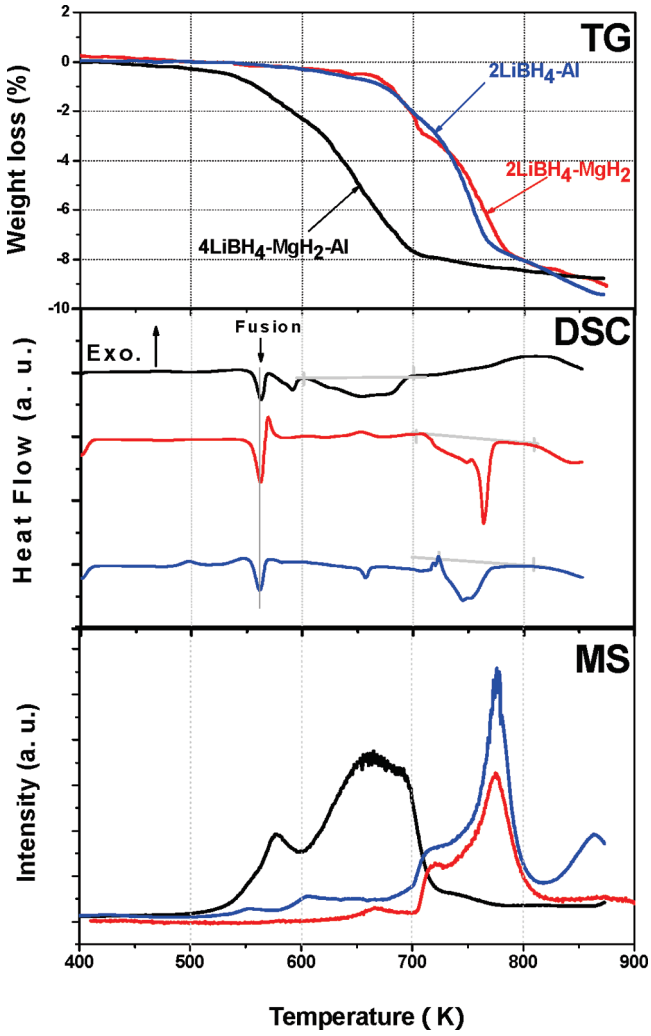

Figure 2. TG−DSC−MS profiles of $4LiBH_4-MgH_2-Al$ (in black), $2LiBH_4-MgH_2$ (in red), and $2LiBH_4-Al$ (in blue) systems, using an argon purge rate of 50 mL $min^{-1}$and a heating rate of 10 K/min.

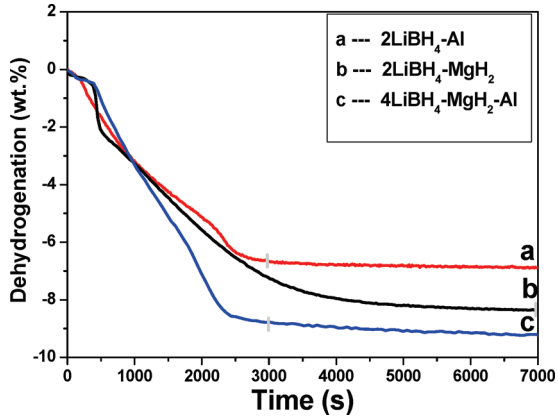

Figure 3. Isothermal dehydrogenation kinetics of $4LiBH_4-MgH_2-Al$, $2LiBH_4-MgH_2$, and $2LiBH_4-Al$ systems under a background pressure of 100 Pa and at 673 K.

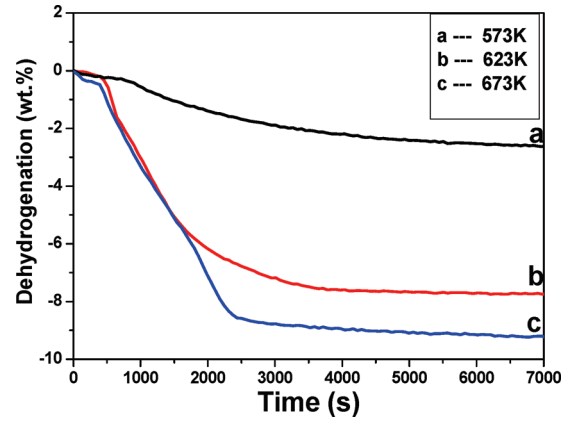

Figure 4. Isothermal dehydrogenation kinetics of $4LiBH_4-MgH_2-Al$ at different temperatures (573, 623, and 673 K) under a background pressure of 100 Pa.

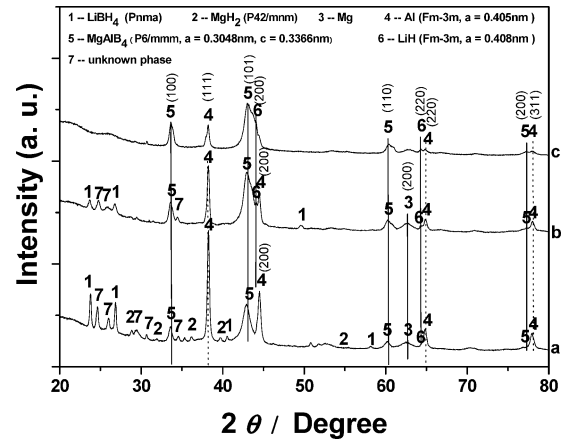

Figure 5. XRD patterns for the $4LiBH_4-MgH_2-Al$ sample dehydrogenated at various temperatures: (a) 573 K, (b) 623 K, and (c) 673 K.

MgB_2 nor AlB_2 phases can be detected in the XRD patterns (Figure 5). Interestingly, a ternary $MgAlB_4$ phase (space group: *P6/mmm*) could be identified in these patterns. It means that the reaction occurring in the present system is not the simple combination of eqs 2 and 3 but a new pathway, which can be expressed by the following equation:

$$4LiBH_4 + MgH_2 + Al \rightarrow 4LiH + MgAlB_4 + 7H_2 \quad (5)$$

Although the identified reaction differs from the hypothesized one in eq 4, its theoretical hydrogen capacity still keeps 9.9 wt % H_2. The XRD reflection peaks of $LiBH_4$ were gradually weakened in the patterns with increasing temperature and would thoroughly vanish when the temperature reached 673 K. The phases of LiH and Al possess nearly the same 2θ degrees. The only way to judge the fit of the reflections at the degrees (2θ) of 38.3° and 44.5° is by means of the intensity ratio of their peaks. The Al phase usually exhibits a strong peak at 38.3° and a relatively weaker one at 44.5°, whereas the LiH is opposite. It can be confirmed that some Al still exists in the sample when the temperature is at 673 K. However, with the temperature increasing to 673 K, the intensity of the Al reflection peaks is obviously weakened in the XRD pattern of Figure 5. This suggests that Al is gradually involved in the reaction with $LiBH_4$ and MgH_2. The remaining Al in the dehydrogenated $LiBH_4-MgH_2-Al$ system indicates that the reaction at this temperature is not thoroughly executed. It indicates that the dehydrogenation is not a fully completed reaction.

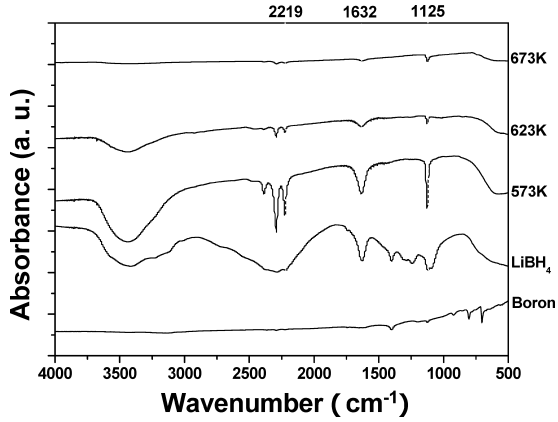

Figure 6. FT-IR spectra for the $4LiBH_4-MgH_2-Al$ sample dehydrogenated at various temperatures (573, 623, and 673 K).

As is known, the sample chamber is a closed system for the isothermal dehydrogenation kinetics. Even though the initial state is nearly vacuum (100 Pa), the pressure in the chamber would still increase gradually in the process of dehydrogenation. The final pressure in the chamber could attain 0.1 MPa. The increasing pressure may inhibit the complete dehydrogenation of some samples. More than likely, the dehydrogenation of the $LiBH_4-MgH_2-Al$ sample is very sensitive to the hydrogen pressure. That should be the reason why the released hydrogen amount closest to a reaction completion but does not attain the theoretical value.

The formation of elemental boron can hardly be identified by analysis of the XRD patterns in Figure 5. As is known, the boron phase in the dehydrogenated samples of $LiBH_4$-relevant is usually amorphous.[15] The FT-IR spectra are thereby used to detect the characterized frequencies of B−B spectra in amorphous boron.[29] In Figure 6, however, still no characterized vibration signal corresponding to the amorphous boron can be detected in each IR spectrum of the as-dehydrogenated samples. It means that the formation of the boron phase can be effectively suppressed by means of doping MgH_2-Al additives. As is known, the inactive properties of elemental boron usually leave it unfavorable for the process of rehydrogenation of $LiBH_4$ and its relevant composites.[20,21] The dehydrogenation products without boron likely play a positive role in the enhancement of the rehydrogenation performance.

Metallic Mg can be characterized in the XRD patterns (Figure 5) of the system dehydrogenated at 573 and 623 K but nearly vanishes when the temperature increases to 673 K. The yielded Mg is likely due to the partial decomposition of MgH_2. Because no AlB_2 or B can be detected in the XRD and FTIR results, we can exclude the possibility that Mg reacts with AlB_2 or Al−B and generates $MgAlB_4$. The possibility of alloying with Al is also excluded because no Mg−Al binary alloy is observed. For the almost disappeared Mg, it is most likely that the enhanced kinetics of the exchange reaction in eq 5 effectively inhibited the self-decomposition of MgH_2.

The $P-C-T$ measurements were performed on the $4LiBH_4-MgH_2-Al$ sample for its dehydrogenation at 623, 653, and 673 K. In Figure 7, sloping plateaus ranging from 0.01 to 5 MPa were observed in the isotherms.

The desorption enthalpy change (ΔH) and entropy change (ΔS) of the system can be calculated by means of the temperature-dependent equilibrium pressure (P_{H_2}) van't Hoff equation

$$\ln P_{H_2} = 1/T(-\Delta H/R) + \Delta S/R \quad (6)$$

where T is the absolute temperature and R is the gas constant. A van't Hoff plot (natural logarithm of the equilibrium pressure versus the inverse of the absolute temperature) is shown in Figure 7 where the desorption equilibrium pressure is designated as the pressure value at the median of dehydrogenation capacity. The achieved relationships of $\ln P_{H_2} \sim 1/T$ present a straight line, as shown in the inset of Figure 7, demonstrating a satisfied fit ($R^2 = 0.993$) in the van't Hoff equation. On the basis of the fit results, as shown in eq 7, the enthalpy and entropy changes of dehydrogenation are calculated as 57 kJ/mol-H_2 and 75 J/K·mol-H_2, respectively.

$$\ln P_{H_2} = -6923/T + 9 \quad (7)$$

It can be confirmed that the dehydrogenation enthalpy is slightly reduced from pristine $LiBH_4$ ($\Delta H_{de} = 68$ kJ/mol-H_2).[10] Its thermal stability is close to that of the $LiBH_4-Al$ system (59 kJ/mol-H_2).[14] The destabilization by MgH_2-Al coadditives is not as remarkable as that by single MgH_2, which tailors the dehydrogenation enthalpy to 42 kJ/mol-H_2.[19] The plateau pressure dehydrogenated at 673 K confirms the difference. The pressure of the $4LiBH_4-MgH_2-Al$ system represented by the median value (0.274 MPa) is significantly lower than that of the $2LiBH_4-MgH_2$ system (>1 MPa).[19]

The formation enthalpy of $MgAlB_4$ can be roughly estimated on the basis of eq 5 and its change in enthalpy. As is known, the standard formation enthalpies (ΔH_f°) of $LiBH_4$, LiH, and MgH_2 are −190, −90.6, and −76 kJ/mol, respectively.[30] The formation enthalpy value for $MgAlB_4$ was thus calculated as −73.5 kJ/mol. Its thermal stability lies between the two species of MgB_2 (−92 kJ/mol)[30] and AlB_2 (the estimated value varied from −16 to −151 kJ/mol).[31]

3.2. Rehydrogenation of the $LiH-MgAlB_4$ System. The isothermal rehydrogenation is executed after being completely dehydrogenated at 673 K. Figure 8 shows that the saturated capacity of isothermal rehydrogenation increases with the augmentation of temperature. The maximum capacity of ~6 wt % H_2 could be achieved when the temperature is at 673 K. The hydrogen absorption time is significantly reduced when the temperature increases from 573 to 623 K. Figure 8 indicates

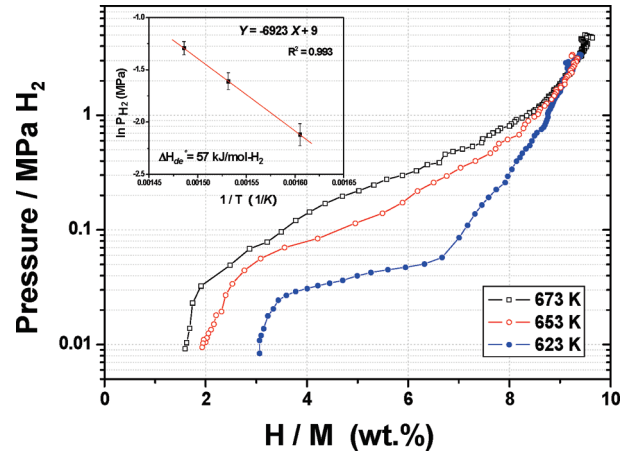

Figure 7. Desorption $P-C$ isotherms at different temperatures (623, 653, and 673 K) of the as-milled $4LiBH_4-MgH_2-Al$ sample without catalyst. The inset is the van't Hoff plot for the dehydrogenated $4LiBH_4-MgH_2-Al$ system. The enthalpy and entropy changes of dehydrogenation are calculated as 57 kJ/mol-H_2 and 103 J/K·mol-H_2, respectively.

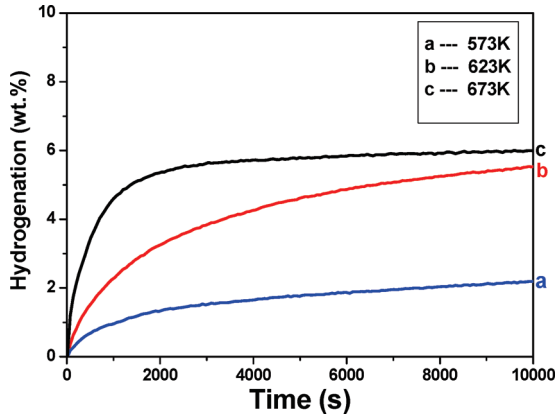

Figure 8. Isothermal rehydrogenation kinetics of the $4LiBH_4-MgH_2-Al$ composite sample obtained at different temperatures (573, 623, and 673 K) under an initial hydrogen pressure of 4 MPa.

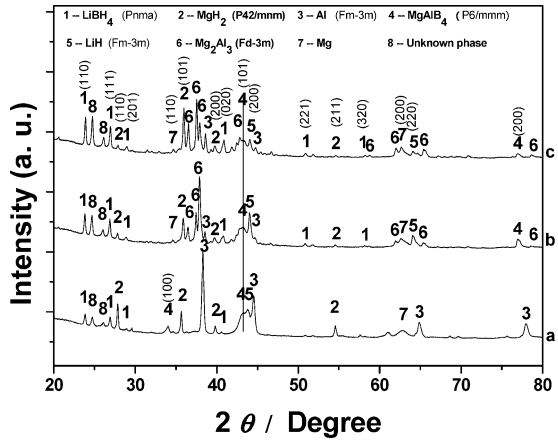

Figure 9. XRD patterns for the $LiH-MgAlB_4$ composite sample hydrogenated at different temperatures: (a) 573 K, (b) 623 K, and (c) 673 K.

that the saturated hydrogenation process of the $LiH-MgAlB_4$ sample can be limited within 4000 s at a temperature of 673 K.

The samples rehydrogenated at various temperatures (573, 623, and 673 K) were investigated by means of XRD measurements. Figure 9, pattern a, shows the XRD reflections of $LiBH_4$, MgH_2, and Al phases in the sample when it was hydrogenated under 4 MPa at 573 K. It demonstrates the reversibility of eq 5 and the recovery of the hydrides at this temperature. However, the recombination of $LiBH_4$ is obviously incomplete at this temperature because such phases as LiH and $MgAlB_4$ still remain in the sample. The identified metallic Mg at 573 K suggests that the backward reaction likely takes place in two steps at a temperature of 573 K:

$$4LiH + MgAlB_4 + 6H_2 \rightarrow Mg + 4LiBH_4 + Al \quad (8)$$

$$Mg + H_2 \rightarrow MgH_2 \quad (9)$$

The coexistence phases of MgH_2 and Mg in the XRD patterns (573−673 K) verify that MgH_2 should be subsequently formed after the yield of Mg. Besides being hydrogenated, the metallic Mg would alloy with Al to form Mg_2Al_3 (space group: $Fd3\bar{m}$) at a temperature of 623 K, as in eq 10. The formed Mg_2Al_3 alloy is extremely stable at 673 K.

$$2Mg + 3Al \rightarrow Mg_2Al_3 \quad (10)$$

$MgAlB_4$ can be identified at 673 K, suggesting that recombination of $LiBH_4$ is not completely finished. Because of the formation of the Mg_2Al_3 alloy instead of MgH_2, the reversible

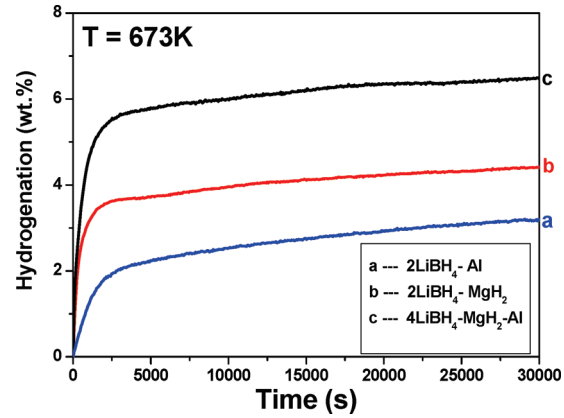

Figure 10. Isothermal rehydrogenation kinetics of $4LiBH_4-MgH_2-Al$, $2LiBH_4-MgH_2$, and $2LiBH_4-Al$ composite samples under an initial hydrogen pressure of 4 MPa and at 673 K.

hydrogen capacity of the $LiH-MgAlB_4$ system will be reduced at the temperatures above 673 K. It verifies that the released amount of 9.4 wt % H_2 is hardly reloaded during the first rehydrogenation.

Figure 10 compares the rehydrogenation kinetics of the $LiH-MgAlB_4$, $LiH-MgB_2$, and $LiH-AlB_2$ systems under the initial pressure of 4 MPa H_2 at 673 K. The saturated hydrogenation capacity (6 wt % H_2) of the $LiH-MgAlB_4$ system is higher than that of the $LiH-MgB_2$ (4 wt % H_2) and $LiH-AlB_2$ (3 wt % H_2) systems. The result indicates that the kinetics of $LiH-MgAlB_4$ is superior to that of the $LiH-MgB_2$ and LiH−Al systems in the recombination of the $LiBH_4$.

4. Conclusions

In the present work, a $LiBH_4-MgH_2-Al$ (4:1:1 mole ratio) composite was synthesized for enhancing its hydrogen de/resorption performances from that of $2LiBH_4-MgH_2$ and $2LiBH_4-Al$ systems.

The major dehydrogenation pathway for the $4LiBH_4-MgH_2-Al$ complex system is identified by X-ray diffraction (XRD) characterizations as $4LiBH_4 + MgH_2 + Al \rightarrow 4LiH + MgAlB_4 + 7H_2$. FT-IR analyses indicate that the additives of MgH_2 and Al can effectively inhibit the formation of elemental boron during the process of dehydrogenation. The nonisothermal measurements performed by thermogravimetry (TG) and differential scanning calorimetry (DSC) show that the dehydrogenation onset temperature is 523 K, which is lowered by more than 100 K from that of $2LiBH_4-MgH_2$ and $2LiBH_4-Al$ systems. The enthalpy and entropy changes of dehydrogenation are identified as 57 kJ/mol-H_2 and 75 J/K·mol-H_2, respectively, by means of pressure−component isotherms and the van't Hoff equation. The dehydrogenation enthalpy is slightly reduced from the pristine $LiBH_4$, demonstrating the destabilization by coadditives of MgH_2 and Al.

As for the rehydrogenation of the $LiH-MgAlB_4$ system, the two-step pathway of $4LiH + MgAlB_4 + 6H_2 \rightarrow Mg + 4LiBH_4 + Al$ and $Mg + H_2 \rightarrow MgH_2$ is identified. However, MgH_2 in the second step cannot be fully recovered because partial Mg formed in the first step would alloy with Al to generate Mg_2Al_3. The isothermal rehydrogenation measurements exhibit significantly enhanced kinetics for the $LiH-MgAlB_4$ system compared with $LiH-MgB_2$ and $LiH-AlB_2$ systems.

Acknowledgment. The authors would like to acknowledge the financial support received from the National Natural Science Foundation of China (Grant Nos. 50901070 and 20833009), the

National High Technology Research and Development Program of China (Grant No. 2007AA05Z120), and the National Basic Research Program of China (Grant No. 2010CB631303). The authors are also grateful to Mr. Markus Karahka from Dalhousie University in Canada for his kind correction on the writing.

References and Notes

(1) Schlapbach, L.; Züttel, A. *Nature* **2001**, *414*, 353–358.
(2) Schüth, F.; Bogdanović, B.; Felderhoff, M. *Chem. Commun.* **2004**, *20*, 2249–2258.
(3) Bogdanović, B.; Ritter, A.; Spliethoff, B. *Angew. Chem., Int. Ed. Engl.* **1990**, *29*, 223–234.
(4) Bogdanović, B.; Schwikardi, M. *J. Alloys Compd.* **1997**, *253−254*, 1–9.
(5) Chen, J.; Kuriyama, N.; Xu, Q.; Takeshita, H. T.; Sakai, T. *J. Phys. Chem. B* **2001**, *105*, 11214–11220.
(6) Muller, A.; Havre, L.; Mathey, F.; Petit, V. I.; Bensoam, J. U.S. Patent 4,193,978, 1980.
(7) Chen, P.; Xiong, Z. T.; Luo, J. Z.; Lin, J. Y.; Tan, K. L. *Nature* **2002**, *420*, 302–304.
(8) Xiong, Z. T.; Wu, G. T.; Hu, J. J.; Chen, P. *Adv. Mater.* **2004**, *22*, 1522–1525.
(9) http://www1.eere.energy.gov/hydrogenandfuelcells/mypp/pdfs/storage.pdf.
(10) Züttel, A.; Wenger, P.; Rentsch, S.; Sudan, P.; Mauron, Ph.; Emmenegger, Ch. *J. Power Sources* **2003**, *118*, 1–7.
(11) Züttel, A.; Rentsch, S.; Fischer, P.; Wenger, P.; Sudan, P.; Mauron, Ph.; Emmenegger, Ch. *J. Alloys Compd.* **2003**, *356−357*, 515–520.
(12) Aoki, M.; Miwa, K.; Noritake, T.; Kitahara, G.; Nakamori, Y.; Orimo, S.; Towata, S. *Appl. Phys. A: Mater. Sci. Process.* **2005**, *80*, 1409–1412.
(13) Kang, X. D.; Wang, P.; Ma, L. P.; Cheng, H. M. *Appl. Phys. A: Mater. Sci. Process.* **2007**, *89*, 963–966.
(14) Friedrichs, O.; Kim, J. W.; Remhof, A.; Buchter, F.; Borgschulte, A.; Wallacher, D.; Cho, Y. W.; Fichtner, M.; Oh, K. H.; Züttel, A. *Phys. Chem. Chem. Phys.* **2009**, *11*, 1515–1520.
(15) Au, M.; Jurgensen, A. *J. Phys. Chem. B* **2006**, *110*, 7062–7067.
(16) Au, M.; Jurgensen, A.; Zeigler, K. *J. Phys. Chem. B* **2006**, *110*, 26482–26487.
(17) Meisner, G. P.; Scullin, M. L.; Balogh, M. P.; Pinkerton, F. E.; Meyer, M. L. *J. Phys. Chem. B* **2006**, *110*, 4186–4192.
(18) Pinkerton, F. E.; Meyer, M. S.; Meisner, G. P.; Balogh, M. P. *J. Phys. Chem. B* **2006**, *10*, 7967–7974.
(19) Vajo, J. J.; Skeith, S. L. *J. Phys. Chem. B* **2005**, *109*, 3719–3722.
(20) Bosenberg, U.; Doppiu, S.; Mosegaard, L.; Barkhordarian, G.; Eigen, N.; Borgschulte, A.; Jensen, T. R.; Cerenius, Y.; Gutfleisch, O.; Klassen, T.; Dornheim, M.; Bormann, R. *Acta Mater.* **2007**, *55*, 3951–3958.
(21) Barkhordarian, G.; Klassen, T.; Dornheim, M.; Bormann, R. *J. Alloys Compd.* **2007**, *440*, L18–L21.
(22) Yang, J.; Sudik, A.; Wolverton, C. *J. Phys. Chem. C* **2007**, *111*, 19134–19140.
(23) Zhang, Y.; Zhang, W. S.; Wang, A. Q.; Sun, L. X.; Fan, M. Q.; Chu, H. L.; Sun, J. C.; Zhang, T. *Int. J. Hydrogen Energy* **2007**, *32*, 3976–3980.
(24) Gross, A. F.; Vajo, J. J.; Van Atta, S. L.; Olson, G. L. *J. Phys. Chem. C* **2008**, *112*, 5651–5657.
(25) Kim, Y.; Reed, D.; Lee, Y. S.; Lee, J. Y.; Shim, J. H.; Book, D.; Cho, Y. W. *J. Phys. Chem. C* **2009**, *113*, 5865–5871.
(26) Jin, S. A.; Shim, J. H.; Cho, Y. W.; Yi, K. W.; Zabarac, O.; Fichtner, M. *Scr. Mater.* **2008**, *58*, 963–965.
(27) Jin, S. A.; Lee, Y. S.; Shim, J. H.; Cho, Y. W. *J. Phys. Chem. C* **2008**, *112*, 9520–9524.
(28) Her, J. H.; Yousufuddin, M.; Zhou, W.; Jalisatgi, S. S.; Kulleck, J. G.; Zan, J. A.; Hwang, S. J., Jr.; Bowman, R. C.; Udovic, T. J. *Inorg. Chem.* **2008**, *47*, 9757–9759.
(29) Binnenbruck, H.; Werheit, H. *J. Less−Common Met.* **1976**, *47*, 91–96.
(30) http://webbook.nist.gov/chemistry/form-ser.html.
(31) van Setten, M. J.; Fichtner, M. *J. Alloys Compd.* **2008**, *477*, L11–L12.

JP9068366